UWB UHF DUAL-POLARIZATION ICE-PENETRATING RADAR: DEVELOPMENT AND ANTARCTIC FIELD TEST

S. Kaundinya¹, L. Taylor¹, U. Dey Sarkar¹, V. Occhiogrosso¹, H. Mai¹, A. Hoffman², K. Christianson², J. Paden¹, A. Paden¹, and F. Rodriguez-Morales¹

1. Center for Remote Sensing and Integrated Systems, University of Kansas, USA

2. Department of Earth and Space Sciences, University of Washington, USA

ABSTRACT

We present the design and field test results for a 600 to 900 MHz polarimetric ice penetrating radar that can be operated on the ground or from an airborne platform. This system is part of a development to build a dual band (VHF/UHF) polarimetric ice sounding radar suite. The VHF radar operates over 140-215 MHz and is essentially a modified version of the multi-channel 3D imaging system reported in [1]. The UHF radar, the focus of this work, is an adaptation of the CReSIS Accumulation Radar, which operates from 600 to 900 MHz [2]. The radar system uses a custom-designed, dual-polarized 4x4 antenna array with increased peak and average transmit power levels, which together provide additional sensitivity with respect to prior system renditions. The UHF radar incorporates a new receiver [3] that uses controlled analog compression via RF limiters to increase the instantaneous dynamic range. We designed the instrument setup to be towed by snowmobiles and operated at nominal speeds of 4 to 8 m/s. The relatively slow motion helps improve SNR through an increase in coherent averaging due to the longer dwell time. Although the focus of the field test is on ground-based work, the electronics are designed to also support airborne operation.

Index Terms— Radar, radioglaciology, UHF, polarimetric, antenna array

1. INTRODUCTION

Radar sounders can map the geometry or shape of internal layers in an ice sheet, but the layer shape is the integration of many physical processes over time that make it hard to unambiguously relate layer shape to current ice sheet processes and model results. In the past decade, ApRES [4] has been used to infer relative vertical velocity of the layers. It is a stationary radar that takes interferometric measurements over time, measuring the change in the range to the layers. Unlike layer shape, vertical velocity can be directly computed by ice flow models and hence is a good tool to compare measured and simulated ice flow. We have demonstrated recently that these interferometric measurements can be done from a mobile platform as long as the spatial baseline is accounted for and the direction of arrival to the target must be known to do the compensation.

To this end, the dual-band concept combines a 3D imaging (i.e., direction finding) VHF radar with the UHF

radar described in this work. The VHF radar provides a way to measure the direction of arrival and the UHF radar utilizes a higher frequency to improve the phase sensitivity of the measurement.

Additionally, the antennas for both radars were designed for polarimetric operation to 1) improve the signal to noise ratio for signal energy lost due to depolarization in anisotropic ice, and 2) to infer properties about the ice crystal fabric orientation which will help infer both past ice stress and present-day ice dynamics.

This paper is organized as follows. Section 2 provides a brief overview of the radar electronics. Section 3 discusses the antenna array design. Section 4 reviews the field measurement configuration. Section 5 presents preliminary field results. Section 6 provides some concluding remarks and discusses future work.

2. RADAR SYSTEM OVERVIEW

The UHF radar system is composed of four main sections: digital, power conditioning, RF, and antennas.

Table 1 offers a summary of the system parameters while Figure 1 presents a simplified block diagram of the radar system. The digital section consists of clock generation and distribution circuitry, two waveform generators, two digitizers, a central timing unit for digital IO and radar timing, a precision dual-antenna GPS receiver, and a control computer and network switch. The clock generation circuitry produces a 2.0 GHz sampling clock signal locked to a stable 10-MHz reference signal by an oven oscillator. The waveform generators synthesize chirp waveforms in the 600 to 900 MHz range at 2 GS/s for the H and V antennas respectively; only one transmitter operates at any given moment in time. The digitizers, operating at 1 GS/s after dividing the 2 GHz clock by two, directly capture coherent radar returns from the H and V polarizations in the second Nyquist zone. Onboard pre-summing is used to reduce data rates (e.g., 10 MB/sec typical) during multi-hour acquisitions. The central timing unit controls data flow and provides input/output ports to control RF switches and record time stamps from the GPS receiver. A small computer running a graphical user interface controls the digital section and records data onto a small solid-state drive (SSD). The power conditioning section filters the power from an external AC generator and produces individual DC

voltage rails, as required for the various sub-components within the radar.

The RF section is composed of two (one for each polarization) transmit/receive (T/R) modules, pre-select band-pass filters and directional couplers; and two analog receiver modules. The T/R modules have a driver amplifier, a high-power amplifier, and a T/R switch to alternate the antenna function between transmission and reception for both polarizations. The power amplifiers can produce up to ~1600 W peak per channel (although for this field season we were limited to ~400 W). The analog receiver has two switching stages controlled by the central timing unit on a per-pulse basis. In the high gain switching state, the receiver maximizes the radar's sensitivity for capturing returns from the ice bottom and deep internal reflecting horizons (IRHs). In the other switching states, the receiver gain is reduced, and larger signals can be captured without saturating the receiver. There is also a mode to capture the signals from the reflect port of the antenna feed network directional coupler connected to the output of the T/R module. In this mode, the radar receiver is in a very low gain state that allows it to receive the surface return and shallow IRHs even when operating from the ground. The RF and digital section are separated into two levels within the main radar chassis, as done in [1], to maximize isolation between them.

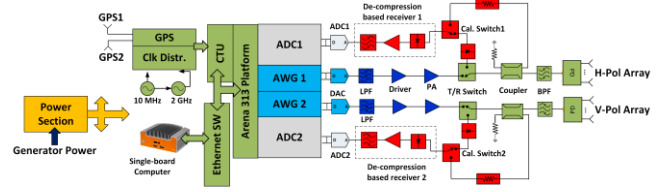


Figure 1: Simplified radar block diagram.

Table 1: Summary of operating parameters

Parameter	Value
Operating frequency range	600 - 900 MHz
Vertical resolution in ice	45 cm (1.6 window factor)
DAC Sampling rate	2 GSPS
ADC sampling rate	1 GSPS
ADC resolution	14 bits
Receiver channels	2 (V, H)
Transmit channels	2 (V, H)
Peak transmit power	1600 W
Pulse repetition frequency	Programmable; ~10 kHz
Transmit pulse duration	Programmable; ~1-10 μs

3. SLED ANTENNA ARRAY

A 16-element antenna array in a 4x4 grid is designed for the UHF system. Figure 2 shows the antenna array assembly diagram including the power divider network to feed the array. The dimensions of the sled are $1.2 \text{ m} \times 0.93 \text{ m} \times 0.28 \text{ m}$ and weighs 105 kg fully assembled with all feed cables. It is constructed of Baltic birch plywood and the underside is lined with HDPE plastic to reduce friction on

snow. A pair of height adjustable keels help prevent it from sliding sideways as it moves forward. The heading and pitch of the sled are measured using a dual antenna GPS setup.

Each antenna element is a dual-polarized dipole antenna with loop radiators, aperture coupled balun, and third-order matching network [5]. An aluminum sheet is glued to a wooden panel and placed at a height of 10 cm from the elements, which corresponds to a quarter-wavelength at the center frequency (750 MHz).

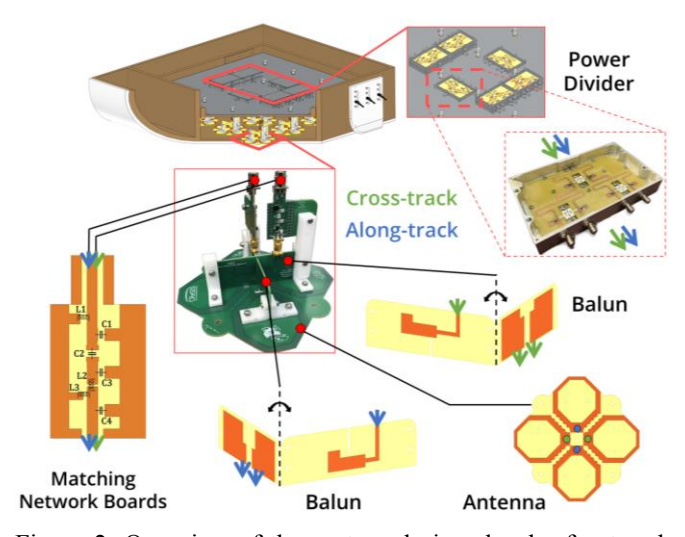


Figure 2: Overview of the custom designed radar front-end showing a cross-sectional view inside the sled, close-up of the power divider network, and exploded view of the antenna assembly.

The power divider network for each polarization consists of five custom-designed 1:4 Wilkinson-based, microstrip power dividers [6] (Figure 2). Each along-track column of antenna elements is connected to one divider and cascaded with the final one using a 12.5 cm Minicircuits 141-SM series coaxial cable.

A set of impedance matching network boards are designed using the process shown in the flowchart in Figure 3. The conventional process for final tuning involves swapping components in the fully assembled setup in the anechoic chamber. Typically, it is time-consuming and onerous to achieve uniform performance across all elements. Hence, this real-time impedance tuning method was developed to streamline the process and achieve reliable performance across elements.

Figure 4 (left) shows the active return loss plots relative to along- and cross-track polarization of antenna element #1 (outermost in grid). Each plot shows the impedance match of the array at vital stages in the tuning process. The solid green trace represents the measurement of the tuned sled array. The final measurement for the along-track elements shows good array impedance matching for the 600 to 900 MHz band. The cross-track elements can be improved by tuning the balun design and further optimizing the matching network.

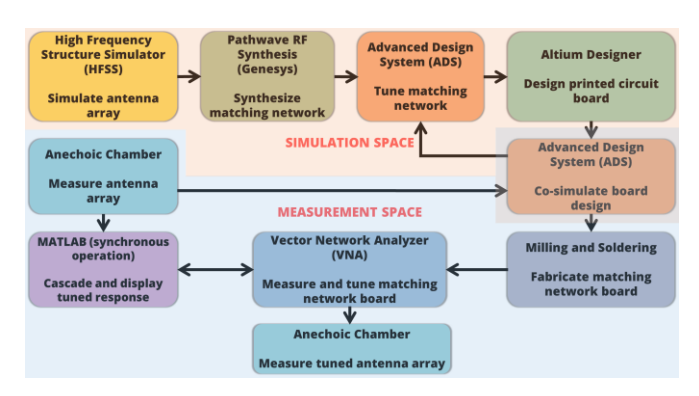


Figure 3: Flowchart of the developed antenna array impedance tuning method to streamline process and achieve reliable performance.

Figure 4 shows the cross-track, normalized radiation pattern of the array. Comparison of simulation and measurement for the low, center, and high frequency shows excellent agreement. The measured half-power beamwidths are 33.7°, 26.7°, and 24° respectively and the average nadir gain is approximately 12.5 dB. It is important that the minimum side-lobe level is less than 10 dB as it improves the effect of clutter reduction and hence clarity of deeper layers.

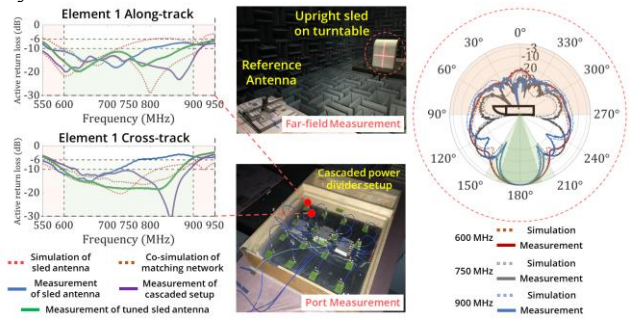


Figure 4: (Left) Active return loss of the array at key stages in the tuning process, (Middle) photos of the sled array in the anechoic chamber during measurements, and (Right) cross-track normalized radiation pattern of the array with antenna sled orientation overlaid in black.

4. FIELD MEASUREMENT CONFIGURATION

The radar and antenna array sleds were towed via snowmobile, as shown in Figure 5 below. The antenna sled was towed by a static line attached to the Siglin sled, while the Siglin sled connected to the snowmobile directly using the towing hitch assembly. Power for the radar electronics was provided by a 2 kW 110 VAC generator. The radar chassis, with heater, operated inside a foam-insulated high-durability polymer equipment case to improve temperature stabilization and vibration damping. The radar and GPS signals were passed to and from the antenna sled using a

harness consisting of four low-loss coaxial cables, measuring 10 m in length.

Measurements were taken along extended Eastwind Glacier flowlines on the McMurdo Ice Self and across the glacier-shelf transition. Speeds ranging from 15 km/h to 30 km/h were used to traverse flowlines, depending on ice shelf surface smoothness and snowpack density.

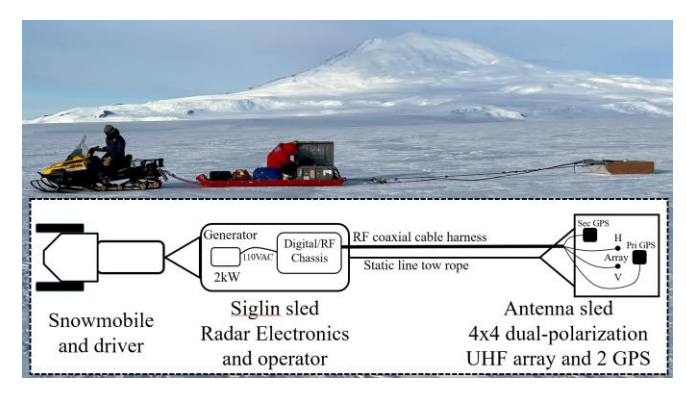


Figure 5: Photograph showing UHF radar system during McMurdo Ice Shelf measurements. The bottom inset diagrams the radar towing arrangement.

5. RESULTS

We deployed the radar system this past field season to two locations. Figure 7 shows the survey lines at each location. We first collected data across the grounding line of the McMurdo Ice Shelf to look at both tidal stresses and begin a time series for analyzing ice flow stress that will be completed during the next field season. The radar was also operated across the West Antarctic Ice Sheet (WAIS) divide and interferometric measurements will be taken during future field seasons here as well. Interferometric processing has not been completed yet, but we present echograms from McMurdo (shallow ice with tidal stressing and fast ice flow) in Figure 6 and WAIS (thick ice with slower ice divide flow) in Figure 8.

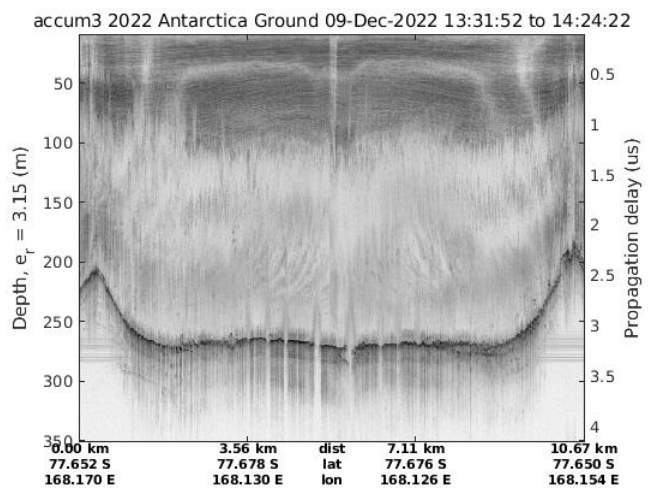
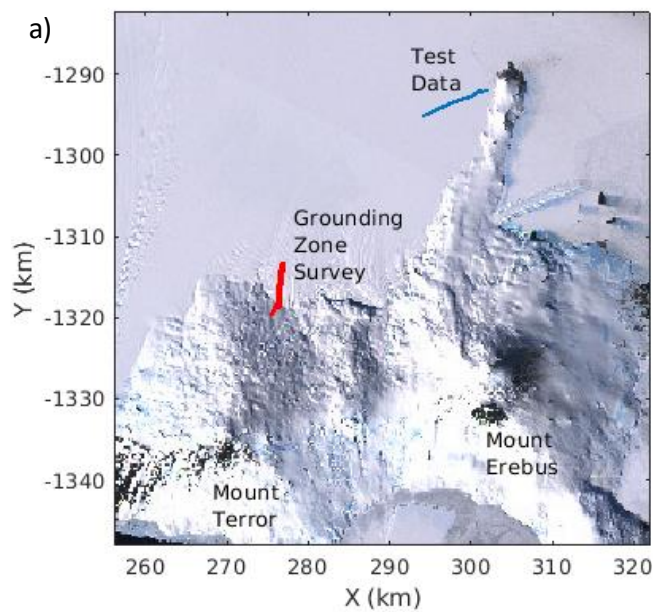


Figure 6: McMurdo Ice Shelf HH echogram.



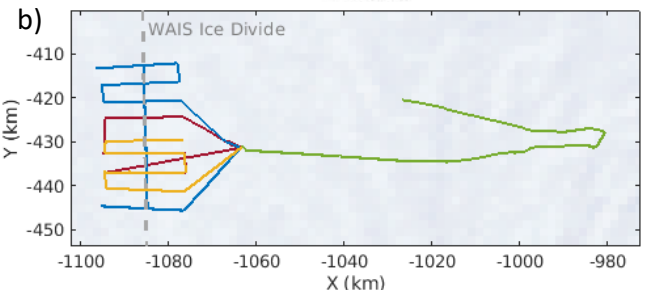


Figure 7: Coverage maps (WGS 84/NSIDC Sea Ice Polar Stereographic South projection) showing survey lines for the a) grounding zone survey (red lines) near McMurdo, Antarctica and b) ice divide survey crossing the WAIS divide indicated by the vertical gray dashed line.

6. CONCLUSIONS

We designed, developed, and deployed a polarimetric 600-900 MHz multichannel radar system. The system is contained in a single box and is capable of ground-based and airborne operation. A ground-based, 16-element, dual-polarized, 4x4, antenna array was designed. The antenna and radar were tested at McMurdo Ice Shelf and at WAIS Divide and preliminary field results are presented. We will be conducting a second field test where multipass measurements will be collected to form interferograms to infer vertical velocity of the internal layers.

REFERENCES

[1] F. Rodriguez-Morales, D. Braaten, H. T. Mai, J. Paden, P. Gogineni, J-B Yan, A. Abe-Ouchi, S. Fujita, K. Kawamura, S. Tsutaki, B. Van Liefferinge, and K.

Matsuoka," A Mobile, Multi-Channel, UWB Radar for Ice Core Drill Site Identification in East Antarctica: Development and First Results," *IEEE J. Sel. Top. App. Earth Obs. Remote Sens.*, Vol. 13, 2020, pp. 4836-4847, 10.1109/JSTARS.2020.3016287.

[2] E. Arnold, C. Leuschen, F. Rodriguez-Morales, J. Li, J. Paden, R. Hale, and S. Keshmiri," CReSIS airborne radars and platforms for ice and snow sounding," *Ann. Glaciol.*, 2019, pp. 1–10. https://doi.org/10.1017/aog.2019.37.

[3] U. Dey Sarkar, S. Kaundinya, L. Taylor, F. Rodriguez-Morales, and J. Paden," Decompression-based receiver design for radar ice sounding applications," submitted to *IEEE International Geoscience and Remote Sensing Symposium*, July 2023.

[4] Nicholls, Keith W., et al. "A ground-based radar for measuring vertical strain rates and time-varying basal melt rates in ice sheets and shelves." *Journal of Glaciology* 61.230 (2015): 1079-1087.

[5] H. T. Mai and F. Rodriguez-Morales, "Broadband Dual-Polarized Planar Antennas for Radar With Printed Circuit Balun," 2021 International Conference on Radar, Antenna, Microwave, Electronics, and Telecommunications (ICRAMET), Bandung, Indonesia, 2021, pp. 89-94, doi: 10.1109/ICRAMET53537.2021.9650456.

[6] Wilkinson, Ernest J. "An N-way hybrid power divider." *IRE Transactions on microwave theory and techniques* 8.1 (1960): 116-118.

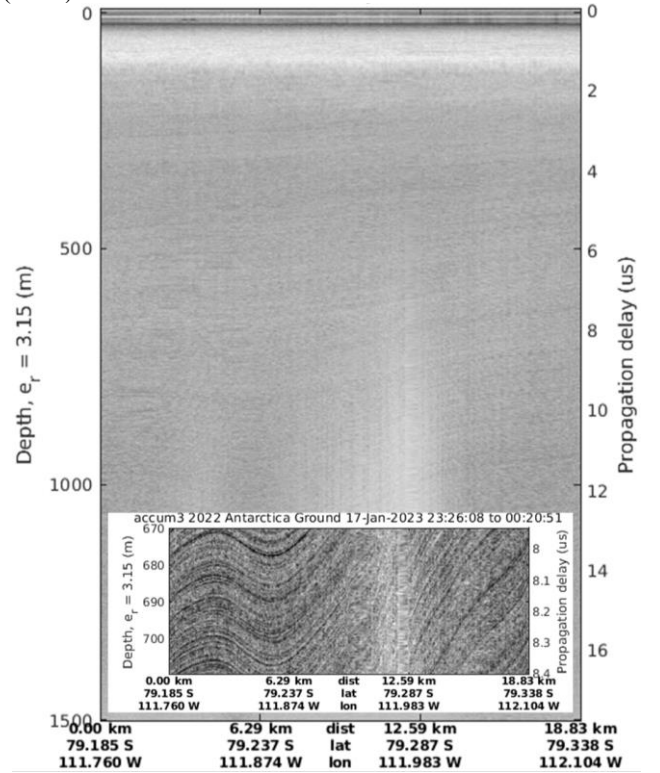


Figure 8: HH echogram collected from the WAIS ice sheet divide. Note that depth resolution is very fine, and the layering is well-defined and relatively flat. The magnified inset shows the layer detail in the image.